arXiv:cond-mat/0302252v1 [cond-mat.supr-con] 13 Feb 2003

Anisotropic Caging of Interstitial Vortices in Superconductors with a Square Array of Rectangular Antidots

L. Van Look,[1] S. Raedts,[1] R. Jonckheere,[2] and V. V. Moshchalkov[1]

[1] *Laboratorium voor Vaste-Stoffysica en Magnetisme, K. U. Leuven Celestijnenlaan 200 D, B-3001 Leuven, Belgium*

[2] *Inter-University Micro-Electronics Center (Imec vzw), Kapeldreef 75, B-3001 Leuven, Belgium*

(Dated: January 26, 2014)

We investigate anisotropy in the vortex pinning in thin superconducting films with a square array of rectangular submicron holes (*"antidots"*). The size of the antidots is chosen in such a way that it corresponds to a saturation number $n_s = 1$, i.e. each antidot can trap at most one flux quantum. Therefore, interstitial vortices, appearing when the magnetic field exceeds the first matching field, are "*caged*" at the interstitial positions by the repulsion from the saturated antidots. We observe an *overall higher critical current* $I_c(H)$ when it is measured parallel to the long side of the antidots than the $I_c(H)$ along the short side of the antidots. Although the pinning force, exerted by the empty antidot on the vortex, turns out to be *isotropic*, our $I_c(H)$ data indicate that the caging force, experienced by the interstitial vortices and provided by the array of saturated antidots, is strongly *anisotropic*.

I. INTRODUCTION

Type-II superconductors (SC's) with nano-engineered pinning arrays are good model systems to study the fundamentals of vortex pinning, since, within the limits of the lithographic process used for their fabrication, they offer the ability to tailor the pinning potential at will.

In SC's with a periodic pinning array (PPA), the vortices form regular geometrical patterns, commensurate with the pinning array, at the integer H_n and fractional $H_{p/q}$ matching fields[1,2]. This strongly reduces the vortex mobility and consequently increases the critical current I_c. These commensurability effects have been intensively studied for square or triangular arrays of antidots[1,2,3,4] or magnetic dots[5,6,7]. The four-fold symmetry in the pinning properties, which is induced by a square PPA, can be broken by using *rectangular* antidots. When no interstitial vortices are present, the critical current $I_c(H)$ is higher in these systems when the current is applied parallel to the long side of the antidots, than when it is applied along their short side, due to a pronounced anisotropy in the vortex-vortex interaction[8].

The size of the antidots determines the saturation number n_s that indicates the maximum flux $n\phi_0$ that can still be trapped by the antidot. When the number n of flux quanta applied per antidot crosses over from $n < n_s$ to $n > n_s$, the pinning potential of the antidots changes from attractive to repulsive.

In the present work, we have made a film with an array of antidots with $n_s = 1$. This implies that *interstitial vortices*, caged by the resultant repulsion of the saturated antidots, appear when the magnetic field exceeds the first matching field. This situation is very different from previous work[8] on rectangular antidots, where no interstitial vortices were present. We investigate the anisotropy of the vortex-vortex interaction between interstitial vortices, and of the caging potential, felt by the interstitial vortices and provided by the repulsive potential of the saturated antidots.

II. EXPERIMENTAL DETAILS

We patterned a SC Pb film in a 5×5 mm^2 cross-shaped geometry (see Fig. 1(a)) to allow electrical transport measurements in two perpendicular current directions. The central part of the cross consists of two 300 μm wide strips containing the square array of rectangular antidots (see dark gray area in Fig. 1(a)). In both strips, the long side of the antidots points in the y-direction. This pattern was prepared by electron-beam lithography in a polymethyl metacrylate/methyl metacrylate (PMMA/MMA) resist bilayer covering the SiO_2 substrate. A Ge(10 Å)/Pb(500 Å)/Ge(200 Å) film was then electron-beam evaporated onto this mask while keeping the substrate at 77 K. A liftoff process in warm acetone finalized the preparation. Figure 1(c) shows an atomic force microscopy (AFM) topograph of a 6×6 μm^2 area of the square antidot lattice with a period of 1.5 μm. The antidots have a rectangular shape (0.5×0.65 μm^2) with rounded corners. As shown in the schematic representation of a unit cell of the array in Fig. 1(b), the superconducting paths between the antidots are 0.85 μm and 1 μm wide, for the x- and y-direction, respectively.

The transport measurements were performed in a ^{4}He cryostat with the magnetic field applied perpendicular to the film surface. The superconducting critical temperature was found to be $T_c = 7.225$ K. To determine the coherence length $\xi(0)$, we measured the linear $T_c(H)$ phase boundary of a reference film, evaporated under identical conditions, without any in-plane nanostructuring. From the $T_c(H)$ slope, and[9]

$$\mu_0 H_{c2} = \frac{\Phi_0}{2\pi\xi(T)^2} = \frac{\Phi_0}{2\pi\xi(0)^2}\left(1 - \frac{T}{T_c}\right), \qquad (1)$$

we find $\xi(0) = 37$ nm. Using the dirty limit ($\ell < \xi_0$)

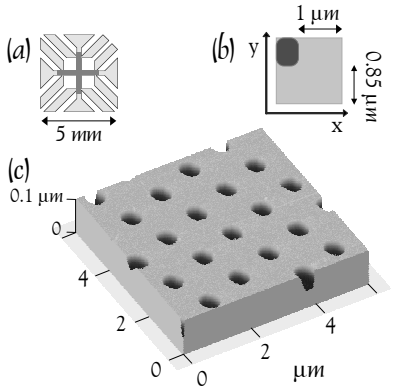


FIG. 1: Layout of the Pb film with a square array of rectangular antidots. (a) Cross-shaped geometry of the sample to allow for transport measurements in the x- and y-direction. (b) Schematic representation of a unit cell (1.5×1.5 μm^2) of the array. (c) Atomic force micrograph of a 6×6 μm^2 area of the antidot lattice.

expression $\xi(0) = 0.865\sqrt{\xi_0 \ell}$ and the BCS coherence length for Pb, ξ_0= 83 nm[10], we determined the elastic mean free path ℓ = 22 nm. We then derive the penetration depth $\lambda(0)$ = 47 nm from the dirty limit expression $\lambda(0) = 0.66\lambda_L\sqrt{\xi_0/\ell}$, using λ_L=37 nm as the London penetration depth[10]. The presence of antidots in a superconducting film increases the penetration depth[11], $\Lambda(0) = \frac{\lambda(0)}{\sqrt{1-2S_a/S_t}} = 56$ nm, where S_a is the area occupied by the antidots and S_t is the total area of the film. The Ginzburg-Landau (GL) parameter $\kappa = \Lambda(0)/\xi(0)$ is therefore $\kappa \approx 1.5 > 1/\sqrt{2} \approx 0.707$. We conclude that the film with the array of rectangular antidots is a type-II superconductor.

III. RESULTS

In Fig. 2, we show the critical current versus field curves $I_c(H)$, normalized to the value at zero field, $I_{co} \equiv I_c(H = 0)$, at two temperatures ($T/T_c = 0.989$ in (a) and 0.992 in (b)). We have used a voltage criterion of $V_{crit} = 100$ μV. The absolute values of the critical current density at zero field measured at $T/T_c = 0.992$ is of the order of $\sim 4 \cdot 10^8 \frac{\mathrm{A}}{\mathrm{m}^2}$ in both directions. The field axis is given in units of the first matching field H_1, the field at which the density of ϕ_0-vortices equals the density of antidots: $\mu_0 H_1 = \Phi_0/d^2 = 9.2$ Oe, with $d = 1.5$ μm the period of the antidot lattice and $\phi_0 = \frac{h}{2e}$ the superconducting flux quantum. For comparison, we have depicted in Fig. 2(c) the $I_c(H)$ curves at $T/T_c = 0.992$ for a superconducting film with a square array (period 1.5 μm) of rectangular antidots with a larger size (0.6×1.15 μm^2)[8]. Due to the presence of the antidot lattice[1,2], both the $I_{cx}(H)$ and $I_{cy}(H)$ data show pronounced maxima at the integer matching fields H_1, $H_2 = 2H_1$, and $H_3 = 3H_1$. Moreover, as it is most clearly seen in the curve measured

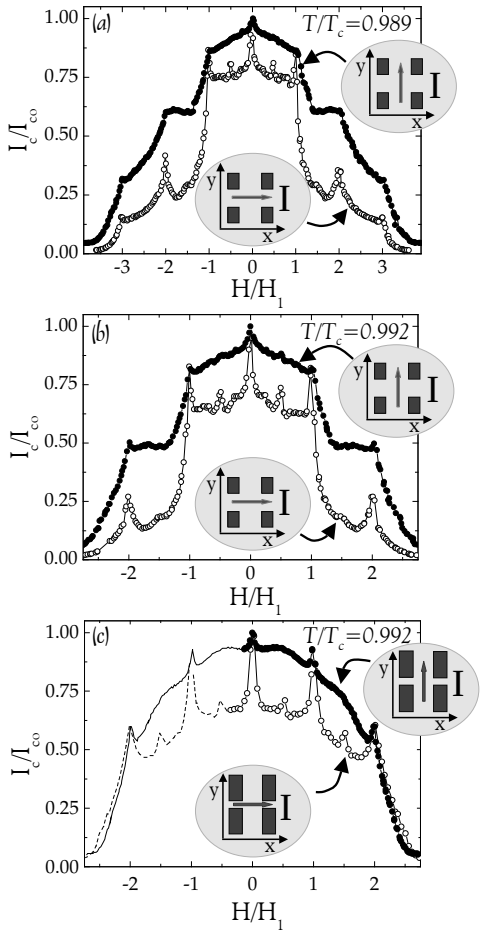


FIG. 2: (a) and (b) Normalized critical currents I_{cx} and I_{cy} as a function of normalized magnetic field H/H_1 for the sample shown in Fig. 1, measured with a current in the x- (open symbols) and the y-direction (filled symbols). Data are presented for two temperatures: (a) $T/T_c = 0.992$ and (b) $T/T_c = 0.989$. (c) $I_{cx}(H)$ and $I_{cy}(H)$ curves at $T/T_c = 0.992$ for a film with a square array of rectangular antidots with a larger size ($0.6 \times 1.15\mu$m^2). The data were obtained for $H > 0$ (open and filled symbols) and then symmetrized for clarity for $H < 0$ (dashed and solid lines) [adapted from Ref.[8]].

with a horizontal current (open symbols in Fig. 2(a-b)), we find a sharp drop in critical current after H_1, indicating the presence of mobile interstitial vortices for $H > H_1$[3]. This means that the antidots can trap at most one flux quantum, in agreement with the calculated saturation number[12] $n_s(T) = \frac{a}{2\xi(T)} = 0.45 \sim 1$ for the temperatures under consideration, where we have used for a the average of the two sides of the rectangular antidot.

Let us first focus on the critical current behaviour in the field range where no interstitial vortices are present, $H \leq H_1$. For these fields, the critical current $I_{cy}(H)$ (filled symbols in Fig. 2) is *considerably enhanced* compared to $I_{cx}(H)$ (open symbols) *except* exactly at the first matching field, where an identical value for $I_c(H_1)$

is found for both current directions. Another striking feature is that rational matching peaks, although clearly present for $I\|\mathbf{x}$ (e.g. at $H/H_1 = 1/4$ and $1/2$), are almost completely suppressed when $I\|\mathbf{y}$. These findings are fully consistent with previous experiments[8] on films with rectangular antidots where the field range, where no interstitial vortices were present, extended up to H_2 ($n_s = 2$)(see Fig. 2(c)).

At higher magnetic fields $H > H_1$, i.e. when interstitial vortices appear in the superconductor with $n_s = 1$, the critical current $I_{cy}(H)$ (filled symbols in Fig. 2(a-b)) is *significantly larger* than $I_{cx}(H)$ (open symbols) for *every* magnetic field, even at the integer matching fields H_2 and H_3. In the film with $n_s = 2$ (Fig. 2(c)), interstitial vortices are not present at H_2. Therefore, the critical current at the second matching field is isotropic, i.e. $I_{cx}(H_2) = I_{cy}(H_2)$. Rational matching peaks are again only found for $I\|\mathbf{x}$, namely at $H/H_1 = 1.5$ (open symbols in Fig. 2(a-b)), whereas no rational matching is found for $I\|\mathbf{y}$.

IV. DISCUSSION

The observed differences in critical current $I_c(H)$ along the two current directions - horizontal and vertical - are due to an anisotropy of the vortex mobility in the sample along the two in-plane directions (x and y). For a certain Lorentz force, this mobility depends on the pinning force experienced by the vortex, and on the vortex-vortex interaction force between neighbouring vortices. Interestingly, since the sample in the present work has $n_s = 1$, the critical current probes the mobility of *two kinds* of vortices, depending on the magnetic field regime, i.e. of the vortices pinned at the antidots and of the interstitial vortices caged in between the saturated antidots. Indeed, at fields below the first matching field H_1, the critical current $I_c(H)$ yields information about the pinning force provided by the rectangular antidots and about the vortex-vortex interaction between vortices pinned at the antidots. At magnetic fields above H_1, the critical current is governed by the mobile interstitial vortices. Therefore, it provides information about the *caging force* produced by the saturated antidots and about the vortex-vortex interaction between two interstitial vortices.

Let us discuss first the regime $H \leq H_1$, where no interstitial vortices are present:

The value of $I_c(H_1)$ is a measure of the single site pinning force of the individual antidots. Indeed, at the first matching field, the vortex-vortex interactions in the highly symmetric vortex lattice (see Fig. 3(a)) cancel out and depinning of the vortices occurs simultaneously once the Lorentz force exceeds the pinning force provided by the antidots. Since the value of the critical current at the first matching field is identical in the x- and the y-direction, i.e. $I_{cx}(H_1) = I_{cy}(H_1)$ (Fig. 2), we conclude that the pinning force exerted by the rectangular antidot on a single pinned ϕ_0-vortex is *isotropic* along the two symmetry-axes of the rectangular antidot. Apparently, the aspect ratio of the rectangular antidots should be much higher in order to produce an anisotropic pinning force[8,13]. Keeping one side of the antidots fixed (semi-axis $b = 0.25$ μm), and taking into account that the coherence length at the considered temperatures is $\xi(T) \approx 0.4$ μm, one would have to construct antidots with an aspect ratio of ~ 8, i.e. with a long semi-axis $a \approx 2$ μm, in order to observe any anisotropy in the pinning force provided by the antidot[13]. The aspect ratio, required to obtain an anisotropic pinning force, is therefore at least a factor of 6 higher than the we have used (see Fig. 1(b)).

The appearance of rational matching features is evidence of a strong vortex-vortex interaction in the direction of the Lorentz force. Since the $I_{cx}(H)$ curve (Lorentz force in the y-direction) shows rational matching and the $I_{cy}(H)$ curve does not, we conclude that the vortex-vortex interaction between vortices pinned at the antidots is stronger in the y- than in the x-direction.

In the field regime $H > H_1$, interstitial vortices are present in our $n_s = 1$ sample. Exactly at the second matching field H_2, a highly symmetric vortex configuration is formed, as is schematically shown in Fig. 3(b). Half of the vortices are strongly pinned at the antidots, the other half is caged in between the saturated antidots. The two vortex species form interpenetrating square lattices. When a current is applied along the x- or y-direction, the interstitial vortices will move first, since they are only weakly pinned[4,14,15]. Therefore, *the critical current at H_2 is a measure of the caging force* provided by the saturated antidots and acting on the interstitial vortices. Since $I_{cy}(H_2) > I_{cx}(H_2)$ (Fig. 2(a-b)), the Lorentz force needed to depin the interstitial vortices is larger in the x- than in the y-direction, and we conclude that the caging force, resulting from the repulsion of the saturated antidots, is *anisotropic*, i.e. stronger in the x- than in the y-direction.

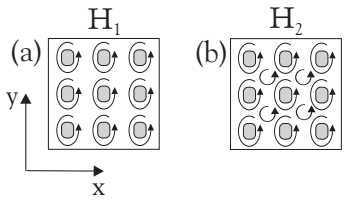


FIG. 3: Schematic presentation of the vortex configuration in the $n_s = 1$ film with a square array of rectangular antidots (a) at H_1, (b) at H_2. Vortices are represented by current arrows.

Moreover, we only find rational matching features in the $I_{cx}(H)$ curves in the field regime $H > H_1$. This indicates that the vortex-vortex interaction between two caged interstitial vortices is also *anisotropic*, i.e. stronger in the y-direction than in the x-direction.

Summarizing our observations, we have found that the vortex-vortex interaction between vortices pinned at

the antidots, as well as between interstitial vortices, is *anisotropic*, i.e. the interaction is stronger parallel to the long side of the rectangular antidots (y-direction). The pinning force, experienced by a caged interstitial vortex and provided by the surrounding saturated antidots is *anisotropic*, i.e. stronger along the short side of the antidots (x-direction). Interestingly, the pinning force provided by the rectangular antidots themselves is *isotropic*.

Most of these features (except for the last, for which we refer to Ref.[8]) can be understood from the geometry of the antidot array. The superconducting strands between the rectangular antidots, where the screening currents of the vortices have to flow, are thinner between the adjacent antidots in the y-direction than in the x-direction (see Fig. 3(a)). Therefore, we expect a stronger vortex-vortex interaction in the y-direction between vortices pinned at the antidots. Moreover, when interstitial vortices are present, it is clear from the schematic presentation of the vortex lattice in Fig. 3(b), that the circulating currents of the interstitial vortices are shielded more in the x-direction, which leads to a weaker vortex-vortex interaction between interstitial vortices in the x-direction. Finally, the anisotropic caging force can be understood if one considers that the rectangular shape of the antidots forces the circulating currents of the vortices trapped inside the antidots to adopt elongated streamlines, rather than circular ones. Since the antidots are placed in a square array, the currents will overlap more in the y-direction (Fig. 3). The caging potential barrier will therefore be higher in the x-direction, i.e. it will be more difficult for an interstitial vortex to pass in between saturated antidots in the x- than in the y-direction.

In other words, due to the application of the array of rectangular antidots, the amount of superconducting material per unit length is smaller for the y-direction than for the x-direction. Consequently, shielding of the magnetic field is poorest in the y-direction, leading to a larger effective penetration depth λ in this direction. Vortices therefore have a stronger vortex-vortex interaction in the y- than in the x-direction.

It is interesting to compare these results with molecular dynamics simulations on a similar system, a *rectangular array* of isotropic pinning sites that can trap at most one vortex[16]. In this system, a different spacing in the x- and y-direction of the pinning sites induces both the anisotropy in vortex-vortex interaction between pinned vortices and in the vortex-vortex interaction between vortices caged at interstitial positions between the saturated pinning sites. The calculated critical current versus field curves for a driving force in the two directions show exactly the same features as found in our $I_c(H)$ measurements.

V. CONCLUSION

We have investigated vortex pinning in a film with a square array of rectangular antidots, focussing on the behaviour of the *interstitial* vortices in this anisotropic environment. Since the antidots we have used have a saturation number $n_s = 1$, i.e. they can trap at most one flux quantum, interstitial vortices appear when the magnetic field exceeds the first matching field H_1. Although the aspect ratio of the antidots is very small, the caging force, provided by the saturated antidots and felt by the interstitial vortices, is stronger along the short side of the antidots. Moreover, we find a weaker vortex-vortex interaction between interstitial vortices in this direction. This leads to an *overall higher* critical current $I_c(H)$ with no rational matching features when it is measured *parallel to the long side* of the antidots. This observation may be important for practical applications of films with a periodic pinning array, since it solves the problem of a reduced critical current density between the matching peaks in $I_c(H)$ at integer H_n and fractional $H_{p/q}$, thus leading to a substantial overall current enhancement due to the presence of the rectangular antidots.

Acknowledgements

This work was supported by the ESF "Vortex" Program, the K.U.Leuven Onderzoeksraad, the Belgian Interuniversity Attraction Poles (IUAP), the Flemish GOA and FWO Programs. We wish to thank M. J. Van Bael and Y. Bruynseraede for helpful discussions.

[1] A. F. Hebard, A. T. Fiory, and S. Somekh, IEEE Trans. Magn. **1**, 589 (1977).
[2] M. Baert, V. V. Metlushko, R. Jonckheere, V. V. Moshchalkov, and Y. Bruynseraede, Phys. Rev. Lett. **74**, 3269 (1995).
[3] V. V. Moshchalkov, M. Baert, V. V. Metlushko, E. Rosseel, M. J. Van Bael, K. Temst, R. Jonckheere, and Y. Bruynseraede, Phys. Rev. B **54**, 7385 (1996).
[4] E. Rosseel, M. J. Van Bael, M. Baert, R. Jonckheere, V. V. Moshchalkov, and Y. Bruynseraede, Phys. Rev. B **53**, R2983 (1996).
[5] Y. Otani, B. Pannetier, J. P. Nozières, and D. Givord, J. Magn. Magn. Mater. **121**, 223 (1993).
[6] D. J. Morgan and J. B. Ketterson, Phys. Rev. Lett. **80**, 3614 (1998).
[7] M. J. Van Bael, J. Bekaert, K. Temst, L. Van Look, V. V. Moshchalkov, Y. Bruynseraede, G. D. Howells, A. N. Grigorenko, S. J. Bending, and G. Borghs, Phys. Rev. Lett. **86**, 155 (2001).
[8] L. Van Look, B. Y. Zhu, R. Jonckheere, B. R. Zhao, Z. X. Zhao, and V. V. Moshchalkov, Phys. Rev. B **66**, 214511 (2002).

[9] M. Tinkham, *Introduction to Superconductivity* (McGraw Hill, New York, 1975).
[10] P.-G. de Gennes, *Superconductivity of Metals and Alloys* (Benjamin, New York, 1966).
[11] A. Wahl, V. Hardy, J. Provost, C. Simon, and A. Buzdin, Physica C **250**, 163 (1995).
[12] G. S. Mkrtchyan and V. V. Shmidt, Sov. Phys. JETP **34**, 195 (1972).
[13] A. Buzdin and M. Daumens, Physica C **294**, 257 (1998).
[14] C. Reichhardt, C. J. Olson, and F. Nori, Phys. Rev. Lett. **78**, 2648 (1997).
[15] K. Harada, O. Kamimura, H. Kasai, T. Matsuda, A. Tonomura, and V. V. Moshchalkov, Science **274**, 1167 (1996).
[16] C. Reichhardt, G. T. Zimányi, and N. Grønbech-Jensen, Phys. Rev. B **64**, 14501 (2001).